

Chapter 8

This chapter deals with the preparation and characterization of three different polyaniline samples, namely, PANI-HCl (synthesized in inorganic acid), PANI-Citric acid (synthesized in organic acid) and PANI-Lemon (synthesized in crude lemon juice: a biological acidic solution). Lemon juice assists to produce specific shape PANI nanostructure (nanorod having dimension ~ 100 nm diameter and ~ 300 - 600 nm length). The self-assembling of polyaniline chains is promoted by the low pKa value of lemon juice, slow kinetics of polymerization, long induction period and the template like effects produced by the matrix molecules. Variation in the intensity ratio for peaks corresponds to benzenoid and quinoid units and blue shift for N=Q=N stretching in FTIR spectrum indicates the distinct molecular structure of PANI-Lemon. PANI-Lemon was successfully applied for the electrocatalytic detection of catechol. The selective interaction of PANI-Lemon with catechol leads to the generation of a new redox center. PANI-Lemon modified carbon paste electrode exhibited high sensitivity ($49.68 \mu\text{A}\mu\text{M}^{-1}\text{cm}^{-2}$), specificity, wide linear range ($5 \mu\text{M}$ - 100 mM), low detection limit ($2.1 \mu\text{M}$) and less response time (2s). In addition, Based on our results, we propose the concept of “Multi-component Template Effects” - a combined templating effect of matrix molecules of the natural extract on the morphology of synthetic polymers and nanoparticles.

8.1 Introduction:

Novel nanomaterials have been prepared by applying specific synthesis protocols. PANI is an excellent and attractive material for various electrochemical and optical applications. Traditionally, PANI is prepared by free radical chemical polymerization in the solution of organic or inorganic acids. Nature of acid and associated anionic dopants bring significant variation in ionic strength, doping level, molecular forces, spatial arrangements and

inter/intra chain charge transport. Different polyaniline nanostructures have been developed, such as – nano-rods, globular, nano-sphere, nano-tubes, nano-sheet, core-shell, thin films and fibers (Zhao et al. 2011; Jabeen et al. 2016; Sapurina et al. 2008; Sen et al. 2016). The degree of oxidation and protonation of PANI chains are very important parameters that control the electrical and optical properties. During doping condition, the imine nitrogen of PANI protonated without changing the number of pi electrons in the chain, and the generated polarons/bipolarons participate in the charge transfer mechanism. In a medium of protonic acid of small molecular size (HCl and H₂SO₄), a globular morphology was observed (Ghadimi et al. 2002).

Hung et al. reported that the morphology of polyaniline depends upon the functionality and substitution of associated anions of organic acids. The morphology of polyaniline depends upon the functionality and substitution of associated anions of organic acids (Huang et al. 1999). The pK_a value of dopant acids strongly correlated with the spectral and redox properties of polyaniline (Hatchett et al. 1999). Macdiarmid et al. described the concept of doping, structural information and conductivity mechanism of the polyaniline doped with nonoxidizing protonic acid (HCl) (Macdiarmid et al. 1987). Structural and morphological characteristics of polyaniline, prepared in HCl and H₂SO₄ have been studied by same researchers. They reported have concluded that significant differences in the induction period and the morphology. The nature of acids and type of associated anionic dopants govern the kinetics of polymerization (Tiwari et al. 2012).

The shape and size of nanomaterials could be easily controlled by directed synthesis, which is an efficient, time-saving, cost-effective and bottom-up approach. Temporary template skeletons direct the spontaneous immobilization/force deposition of the building

blocks of a material. Many solids have been used as hard template structures, such as - membrane, silica, metal oxides and nanoparticles. Materials or their precursors can be filled in the template by the suitable deposition methods, such as sol-gel process, electrochemical polymerization, vapor deposition, casting etc. After deposition, the templates were scaffolded with a suitable remover. Recent advancements reveal that self-assembled structure involves donor/acceptor forces, metal-ligand coordination, hydrogen bonding, π - π stacking, solvophobic repulsion and/or electrostatic forces. Besides these, soft templates were also used for the same purpose. Soft template synthesis (also called as endo-template synthesis) does not have any rigid solid structure (Martin et al. 1996; Wadea et al. 2005; Giz et al. 2000; Holmberg et al. 2004; Chiou et al. 2007). Hard and soft template synthesis have distinct merits and demerits. The hard template provides better control over the shape and size of the products, however, it is a multi-step, complicated, costly and time-consuming procedure. The removal of template structure present in the developed material is a tedious process and requires hazardous chemicals. The soft template has been found to be more efficient, requires less synthetic steps and easy removal of template molecules by the simple process.

Chiou and coworkers reported alignment of PANI fibers under controlled deposition on different substrates (Chiou et al. 2008; Pruna et al. 2010). Pruna and coworkers have reported aluminum oxide template assisted electro-polymerization of PANI nanotubes. (Montilla et al. 2009), reported template assisted growth of PANI by using porous sol-gel films (Olad et al. 2012). Porosity of polyaniline is an important factor. It depends on synthesis process parameter, additive used and the refining steps (Jabeen et al. 2016; Liu et al. 2017; Fryczkowski et al. 2013; Lin et al. 2006; Anbalagan et al. 2016). Doping-dedoping-

redoping is a convenient way to achieve specific property and desired level of doping (Li et al. 1998).

Scientists and environmental activists are advocating green manufacturing protocols, environment-friendly chemicals and clean technologies for the global sustainable development. Conventional doping of PANI with HCl is liable to dedoping and the evolution of HCl on evaporation may damage the device. Industrial production of PANI using strong inorganic acids results in discharge of corrosive acidic waste in the water bodies which has an adverse impact on the ecosystem. Lemon juice is environment-friendly and biocompatible acidic solution. It is a low-cost material for the green synthesis of PANI. Lemon juice consists of many weak organic acids, which facilitate slow polymerization reaction and directional alignment of polyaniline chains. Helali et al. studied the important characteristics of lemon juice having composition as: moisture (89.7%), total solid (10.3%), total suspended solids (8.7%), total sugar (4.2%), pH (2.54), citric acid (0.53%), vitamin-C (35.08 mg/100g), a sugar:acid ratio (7.97%) and ash (0.39%). Naseem and coworkers reported environment-friendly oxidative chemical polymerization of PANI using lemon juice. The main objective of this research work is to study the spectroscopic, morphological and electrochemical characteristics of the three PANI samples (PANI-Lemon, PANI-HCl, and PANI-Citric acid) and use them as electrochemical sensor.

Many phenolic compounds have been widely used in different chemical industries. Catechol or pyrocatechol or 1,2-dihydroxybenzene (molecular formula $C_6H_6O_2$) is commonly used in medicines, cosmetics, dye developers, pesticides/fungicides and antioxidants. It is released into the environment during its manufacturing and uses. Hence, its detection is very important for environmental protection and public health. Its exposure may cause many

metabolic disorders, e.g. Atherosclerosis, Parkinson, Alzheimer, Diarrhea, depression of central nervous system, gastrointestinal, respiratory, and cardiovascular problems. Enzymatic and nonenzymatic detection of catechol has been reported by many researchers (Alshahrani et al. 2014; Chandra et al. 2013; Chena et al. 2009; Lakshmi et al. 2009; Fu et al. 2014; Tanget al. 2008; Mu et al. 2006; Nazari et al. 2015; Sadeghi et al. 2015; Tembe et al. 2008; Sethuraman et al. 2013; Tan et al. 2010; Imato et al. 1993; Xue et al. 2002; Yan et al. 2015; Zhao et al. 2007).

8.2 Experimental:

8.2.1 Materials:

Aniline (Merk India Limited) was purified by vacuum distillation and stored in the refrigerator prior to use. Ammonium peroxodisulphate (APS) was used as received from Qualigens Fine Chemicals (India) and citric acid was purchased from SD fine chemicals. Graphite powder and Nujol oil were purchased from Sigma Aldrich. Lemon juice was freshly extracted from fruits and diluted with double distilled water. All other solutions were prepared in double distilled water. Phosphate buffer solutions (0.1 M PBS) were prepared by using disodium hydrogen phosphate, potassium chloride and potassium dihydrogen phosphate. The pH was adjusted by using hydrochloric acid or sodium hydroxide.

8.2.2 Instrumental Analysis:

Scanning electron microscope (SEM), High resolution-scanning electron microscope (HR-SEM), Transmission electron microscope (TEM) and Atomic force microscope (AFM) techniques were used to explore morphological information. SEM and HR-SEM observations

were performed using Quanta 200, FEI of USA (SEA) PTE Ltd., Singapore and Novanosem respectively, at suitable voltages and magnifications. TEM examination was made using FEI, TECHNAI 20G2 electron microscope at an accelerating voltage of 200KV. AFM characterization was performed with DI Nanoscope IIIa microscope of the LNLS, in non-contact mode, NSC-10-50, » 20N/m at » 260 KHz. The crystalline properties of materials were investigated using Ultima IV X-ray diffractometer with Cu-K α radiation ($\lambda = 1.5404 \text{ \AA}$). The textural properties (surface area, pore size distribution and pore volume) were measured, using a volumetric gas adsorption apparatus at 77 K with a Micromeritics ASAP 2020 physisorption instrument. Before each measurement, the samples were kept at 50°C in vacuum for 12 hours to remove adsorbed foreign molecules. Fourier transform infrared (FTIR) spectra were recorded in the range of 500 - 4000 cm^{-1} , with potassium bromide (KBr) pellets at room temperature, using Perkin Elemer Spectrum version 10.03.05. Electronic structures were analyzed using Varian Carry 100 Bio dual beam UV-Visible Spectrophotometer, in the wavelength region 200 to 900 nm, at a scanning rate 400 nm/min, using the paste of 0.05 g sample in Nujol oil. NMR spectra were obtained by Bruker Ac (250 MHz) spectrometer using DMSO-d₆ solution. Electrochemical studies were carried out using CH600D electrochemical workstation, CH Instruments U.S.A., using a three electrode configuration. Modified carbon paste, Ag/AgCl (saturated with KCl) and Pt wire were used as working, reference and counter electrodes, respectively.

8.2.3 Polymerization of Aniline:

Vacuum distilled aniline was mixed with filtered and diluted lemon juice at the ice-cold temperature. To investigate the effect of lemon juice concentration, two PANI-Lemon

samples were prepared in the solutions of different concentrations; 0.5 % [PANI-Lemon (L)] and 2 % [PANI-Lemon (H)]. Dilute solution of ammonium peroxydisulfate (0.1 M) was used to initiate polymerization reactions. APS was added dropwise in the reaction mixture under stirred condition. After 2 hours of continuous stirring, the reaction mixture was kept undisturbed for 24 hours in order to complete polymerization (Tiwari et al. 2012). The polymerization reactions in lemon juice solution have longer induction period and slow kinetics than others. Initially, the dark brown precipitate was obtained which turned into green color at a later stage (indicating “Emeraldine salt” form of PANI). The polymeric material was filtered and washed several times with 0.1 M HCl solution and final washing was done with acetone. Washing of precipitate removes the residual monomers, the oxidizing agent, oligomers and other soluble contents of lemon juice. PANI-HCl, PANI-Citric acid were prepared as control systems, by following the same procedure in 0.1 M HCl and 0.1 M citric acid solutions, respectively. The obtained materials were weighed and the values of calculated yields were: PANI-HCl: 85%; PANI-Citric acid: 90% and PANI-Lemon: 78%.

8.2.4 Fabrication of carbon paste electrode:

10 mg material was mixed with 100 mg fine quality graphite powder to form a homogeneous paste with 10 μ l Nujol oil. Out of this, 2 mg paste was filled in a glass capillary (2 mm diameter) and a clean copper wire was used for the connection.

8.3 Results and discussion:

8.3.1 The Conceptual Hypothesis Multi-Component Template Effects:

Fascinating nanostructures present in nature motivate scientists to develop novel nanomaterials by adopting the mimic approach. During the biosynthesis of the nanostructure within a natural system (i.e. living cell), the medium consists of many chemical and biochemical molecules. Synergism plays an important role in any biosynthesis. Matrix molecules impact on the morphology of natural nanomaterials. Many research groups have prepared nanoparticles of specific shape and size by using bio-extracts as an environment-friendly option (Gospodinova et al. 1998; Mittal et al. 2013; Akhtar et al. 2013; Ahmed et al. 2015). In the present research work, dilute lemon juice was used for the synthesis of PANI. On comparative analysis of microscopic images its observed that PANI-Lemon has directional synthesis and specific shape nanostructure, whereas PANI-citric acid and PANI-HCl have globular and irregular morphology. Based on our results, we are proposing a hypothetical concept “Multi-component Template Effects” . The important assumptions and aspects are given as (*c.f. DI*). The core idea of this study is to illustrate the template like effect produced by natural molecules on a synthetic system. This concept (in the present format) concerns with the morphological manipulations of synthetic materials, excluding the identity and role of individual molecules and associated changes with them. Further improvements are open for discussion.

8.3.2 Mechanism of Polyaniline Nanorods Formation:

PANI has been prepared by oxidative chemical polymerization of aniline in acidic solution, and the mechanism is well reported in the literature (Jabeen et al. 2016; Sapurina et al. 2008; Sen et al. 2016; Gospodinova et al. 1998). PANI synthesis has three major stages: nucleation, initial growth and secondary growth. Phenazine, a constituent unit of oligomers, act as a

template and it supports self-assembly during secondary growth of PANI. The acidity and nature of associated anions greatly influence the oxidation of aniline. The initial phase (induction period) of polymerization varies in different acids. Anilinium ions combined with monomers and followed chain propagation reaction. Doping is charge-transfer reactions between the organic polymers and ionic dopants, which effectively change the morphology, electrical, electrochemical properties and geometric parameters (bond length and bond angles). The conductivity of PANI depends on the degree of protonation and oxidation, spatial arrangement and chain length (Jabeen et al. 2016; Sapurina et al. 2008; Gautam et al. 2017; Gautam et al. 2016). In the strong acidic solutions, speedy and preferred growth in nucleation leads to the formation of numerous short chains. During the secondary growth phase, these short chains get elongated and entangled as agglomeration. The protonated chains agglomerate in compact coil-conformation due to twist defects between aromatic rings in weakly acidic solution. Low oxidizing agent and rapid movement of monomers could suppress secondary growth and nanofibrous structure produced (Tiwari et al. 2012).

It is very interesting to consider two contrasting effects on the conductivity of PANI. On one hand, strong acid produces highly protonated PANI chains (leads to higher conductivity) but the higher nucleation of PANI could result in irregular agglomerated globular morphology (leads to lower conductivity). Randomly aligned chains have impeded charge transfer due to intra-chain hopping and inter-chain tunneling. On the other hand, weak acid has low protonation level (leads to low conductivity), however, polymer chains align in aregular fashion which results in specific shape nanostructures. The morphological barrier for charge transport could be overcome by spatially arrangements of polymer chains in some regular fashion (leads to better conductivity). We herein propose that protonation level and

spatial arrangement of chains are key factors responsible for the electrical and electrochemical properties of PANI, however under the similar protonating condition, the spatial arrangement is the dominating factor.

The three PANI samples prepared in this work, significantly differ in doping level and type of dopants e.g. PANI-HCl has chloride ions, PANI-Citric acid has citrate anion (as citric acid is a tribasic acid) and PANI-Lemon has multiple dopants (crude lemon juice contains a mixture of organic acids, such as: citric acid, maleic acid, ascorbic acid, trace amounts of tartaric acid, fumaric acid and others). In addition, lemon juice contains minor amounts of glucose and other sugars. The three solutions significantly differ in the acidity (pH of 0.1 M HCl, 0.1 M citric acid and crude lemon juice are 0.8, 3.0 and 2.3, respectively). The lower acidity of dilute lemon juice, multiple bond formation, and slow kinetics facilitated the directional synthesis of the specific nanostructure of PANI. Post-synthesis dedoping/redoping process brings the desired level of doping without perturbing the spatial arrangements of material.

Lemon juice assisted polymerization reaction showed a comparatively longer induction period. Biological molecules, present in the lemon juice, significantly manipulate the polymer-polymer interface. A higher fraction of linear assembled chains is attributed to the electrostatic repulsion between the same charge of chains, and strong interactions between amine and imine groups in adjacent chains via hydrogen bonds. It was observed that induction period was shortened with the increase in the concentration of lemon juice.

The proposed green approach of PANI synthesis used less amount of oxidizing agent and natural acidic medium. As most of the components of lemon juice are water soluble, purity issues could be easily resolved by adopting appropriate washing procedures. During

washing process, most of the soluble contents, residual molecules and side products were separated out from the prepared polymer.

8.3.3 Morphological Studies:

8.3.3.1 SEM Analysis:

SEM images of PANI-HCl, PANI-Citric acid and PANI-Lemon at low different resolutions have been investigated. PANI-Lemon is interconnected polymeric mass having pores/hollow space up to 0.5 to 10 μm (fig. 8.1 C, D). The 3D porous network of nanorods indicates that PANI-Lemon is a low-density material and it may be a suitable host matrix to immobilize nanoparticles/catalyst/bio-molecules for sensor/biosensor application, separation and solid-state doping catalysis.

Molecules of lemon juice put combined effects on the morphology of PANI. Thus, this spatial alignment of chains supports the concept of “Multi-component Template Effects”. Slow nucleation process, linearly aligned chains and template like effects of the matrix have facilitated the formation of polyaniline nanorods. On the other hand, irregular globular morphology of PANI-Citric acid and PANI-HCl was observed, as reported by some earlier researchers (fig. 8.1 A B) (Anbalagan et al. 2016; Ahmed et al. 2015; Gautam et al. 2017; Gautam et al. 2016; Maity et al. 2016; Kulkarni et al. 2004).

HR-SEM images of the PANI samples provides an insight into the morphology of material at the nano level. The three PANI samples exhibited very distinct morphology (*c.f.* D2 A,B,C). PANI-Lemon has rod shape nanostructures with dimension: length ~ 600 nm and diameter ~ 100 nm (magnification 400016 X). We observed longstrip like structures at magnification 2000 X, which is attributed to the combination of nanorods. We inferred that

the systematic orientation of chains facilitated charge transport, rapid proton exchange and better electroactivity.

HR-SEM image of PANI-Lemon (L) and PANI-Lemon (H) reveals that the length of PANI nanorods varies with the concentration of lemon juice. At higher concentration, shorter nanorods were observed due to more concentrated nucleation (*c.f. D2*). PANI-HCl has an irregular lump like morphology, attributed to random agglomeration and coiling of chains (*c.f. D 2A*, the image at 100000 X and 580164 X). Citric acidis tribasic acid and it could crosslink two or more polyaniline chains through ionic bonds. In addition, hydroxyl, carboxylic groupsand bonded water molecule contributed to form a network of hydrogen bonds. These interconnected chains lead to the formation of specific globular porous structure (*c.f. D 2B*, the image at 100000X and 575023 X).

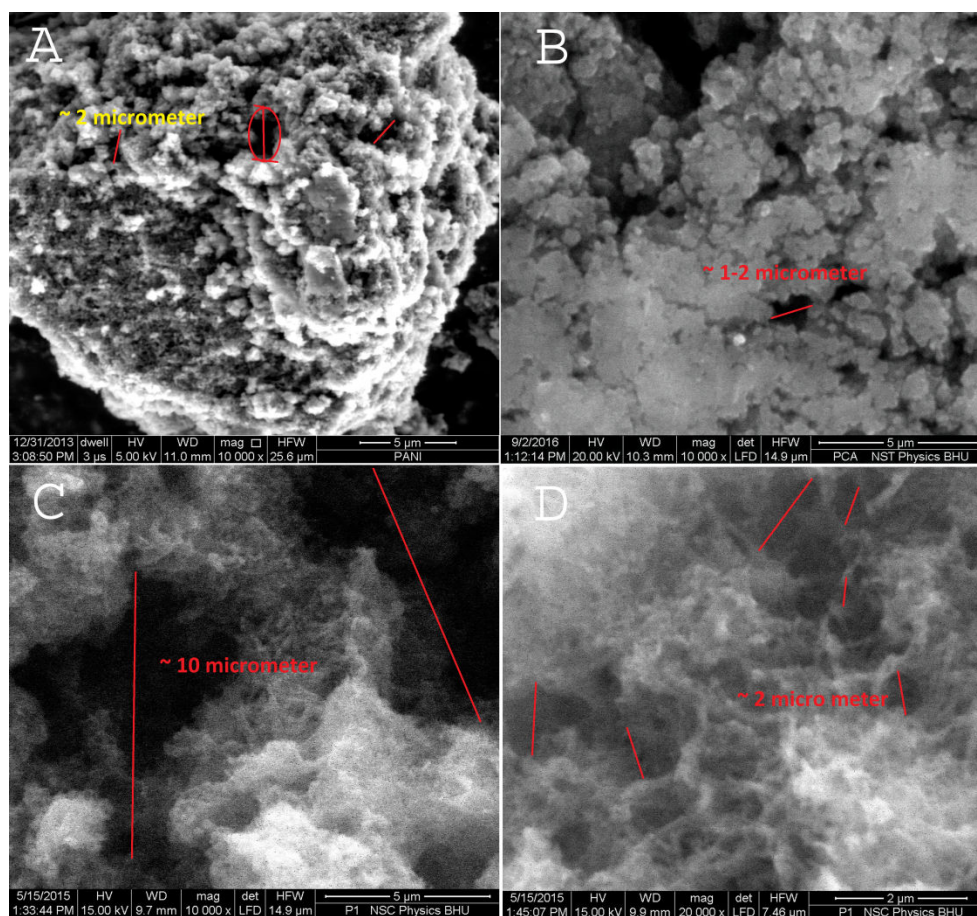


Fig. 8.1 SEM images (A) PANI-HCl (B) PANI-Citric acid (C and D) PANI-Lemon

8.3.3.2 TEM Analysis:

TEM images provide very fine structural information on the nanoscale. PANI-Lemon has interconnected nanorods, sub-nano porosity, regular surface topology with average diameter of a single nanorod 100 - 125 nm and length \sim 300 - 500 nm (fig. 8.1 D, E and F). On the other hand, PANI-HCl and PANI-citric acid have irregular shape and size architecture (fig. 8.1 A, B and C). Tiwari et al. reported the morphological modification by using different acid and additives on PANI-HCl and PANI-H₂SO₄ by TEM images (Tiwari et al. 2012). PANI chains could be oriented by blending with other polymers, by application of high pressure and an electric field. PANI nanofibers have been prepared by electrochemical polymerization (Dhawale et al. 2010). Additional TEM images (at different magnification) and electron diffraction patterns for three PANI samples provide an insight into the morphology and further support the concept of “Multi-component Template Effects” (*c.f.* D3A, B, C). PANI-Lemon has a 3D porous network of porous nanorods (*c.f.* D3C). Zoomed image of the surface, indicated that the nanorod has numerous small porous structures \sim 2-4 nm (*c.f.* D3D). The bright electron diffraction rings confirm that PANI-Lemon has an alignment of chains in an orderly fashion due to various intermolecular forces, multi-component template effects, a network of hydrogen bonds and pi-pi stacking of aromatic rings. X-ray powder diffraction analysis also supported the result (*c.f.* D4). It is to be noted that very few research papers have reported regarding the formation of poly-crystalline PANI (show sharp concentric rings in electron diffraction) (Tiwari et al. 2012). To investigate the surface properties, AFM studies have been carried out for PANI-HCL and PANI-Lemon at the

Chapter 8

nanoscale. AFM image strongly supports the fact that the polymerization in the presence of dilute lemon juice effectively manipulated the morphology, hence rod shape nanostructure is observed, whereas PANI-HCl has aggregated irregular morphology (*c.f. D5*).

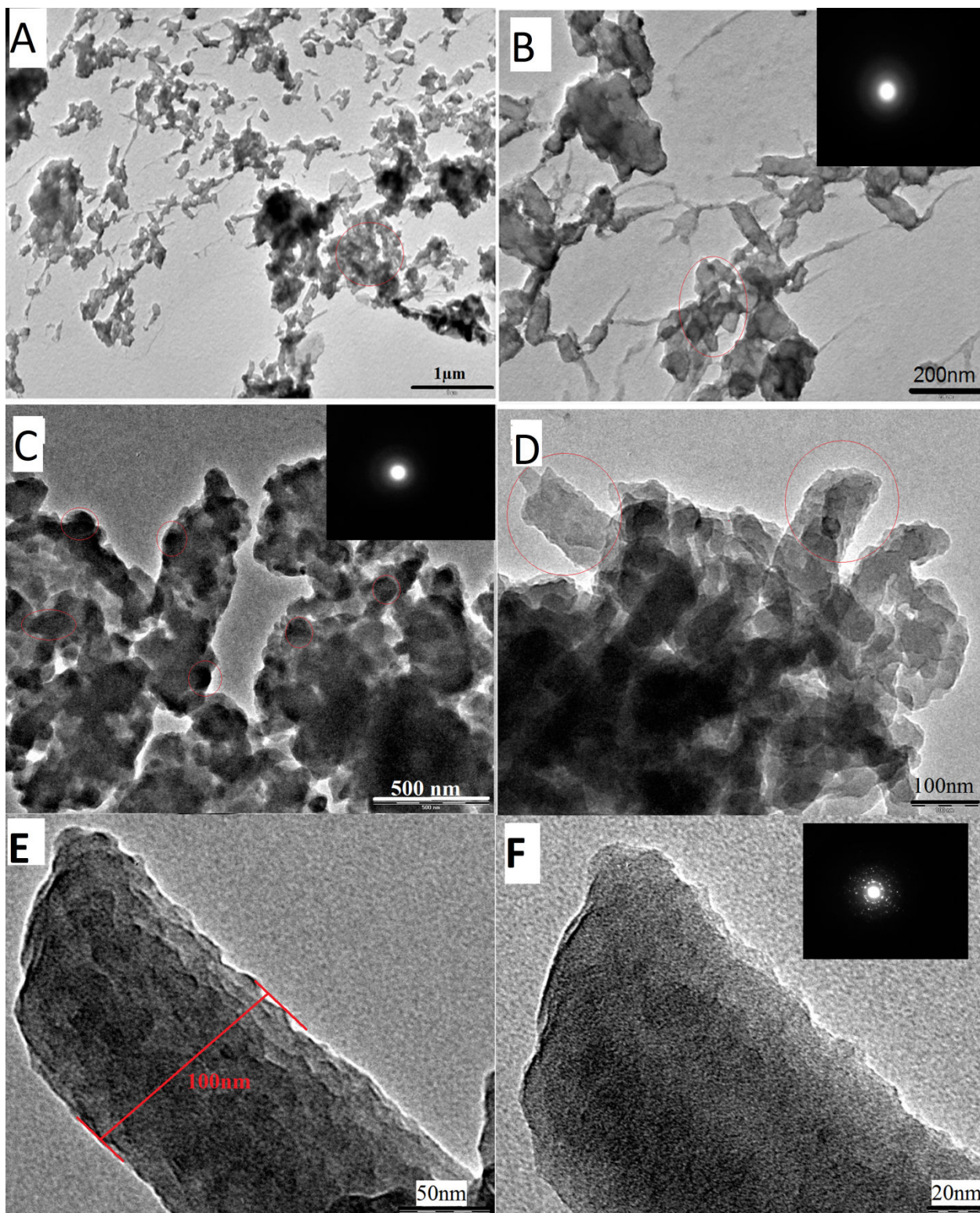


Fig. 8.2 TEM images at different magnifications; PANI-HCl (A, B), PANI-Citric acid, and (C) and PANI-Lemon (D, E and F). Inset-Electron diffraction pattern

8.3.4 Surface Area and Porosity Analysis:

The measurement of surface area, pore size and pore volume are very crucial parameters to optimize the material for many technological applications. The surface area was measured by the theory of Brunauer-Emmet-Teller (BET). Pore size distribution, total pore volume were measured by Brunauer-Joyner-Hallenda (BJH) method. Surface parameters are significantly dependent on the mode of synthesis, the additive used and sample processing for the analysis. Standard procedures have been followed to measure surface parameters for different samples as reported earlier (Gautam et al. 2017; Chowdhury et al. 2008; Sk et al. 2014; Supri et al. 2010).

The adsorption/desorption isotherms, surface area, pore analysis, data point are given as (*c.f. D 6A, B, C*). A sharp increase in the adsorbed volume of N₂ and a hysteresis loop at a high relative pressure ($\approx P/P^0 = 0.95$) are the typical characteristics of mesoporous materials. The specific surface areas calculated by the BET equation for PANI-HCl, PANI-Citric acid, PANI-Lemon (L) and PANI-Lemon (H) were 11.6 m²/g, 10.9 m²/g, 3.7 m²/g and 13.5 m²/g, respectively. The surface area of PANI-Lemon (L) is significantly lower than PANI-HCl and PANI-citric acid. It can be attributed to the formation of the long nanorod and spatial arrangement of small particles. PANI-Lemon (H) (13.5 m²/g) has larger surface area than PANI-Lemon (L) (3.7 m²/g), attributed to the formation of short nanorods (confirmed from HR-SEM images).

PANI-Lemon has lower pore volume and larger pore sizes than PANI-HCl and PANI-Citric acid due to the compact arrangement of PANI particles and strong inter-particle interactions. Lemon juice contains a mixture of organic acid and sugar molecules, and their hydroxyl and carboxylic groups participated in the formation of hydrogen bonds. On comparing the four samples, PANI-Lemon (L) has smallest pore volume, whereas PANI-HCl

has the largest pore volume. Pores with the diameter greater than 10 nm contributed the maximum to the pore volume. The result suggests that PANI-Lemon exhibited type-IV isotherms, which specified the formation of mesoporous structure (2-50 nm). With an increase in concentration of lemon juice, pore diameter and pore volume do not change to a greater extent shown in Table 8.1.

Table 8.1 Pore volume and Pore diameter of PANI-Lemon (L) and PANI-Lemon (H)

	PANI-Lemon(L)	PANI-Lemon(H)
Pore volume	0.02 cm ³ /g	0.08 cm ³ /g
Pore Diameter	17.2 nm	17.6 nm

The presence of hollow space in the polymer matrix is also confirmed from microscopic images. Thus, we infer that PANI-Lemon has mesoporous and rod-shaped structure.

8.3.5 Spectroscopic Analysis:

8.3.5.1 FTIR:

FTIR analysis of polyaniline and its composites has been reported by our group. N–H stretching band ($\sim 3400\text{ cm}^{-1}$), OH stretching of physically adsorbed water molecules (3200 cm^{-1}), CH stretching ($2900\text{--}3100\text{ cm}^{-1}$), presence of benzenoid and quinoid ring vibration (1487 and 1573 cm^{-1}), to C–N/C=N (1305 cm^{-1}), N=Q=N produce sharp and strong bands (1130 cm^{-1}) are CCC ring in-plane deformation due to 1240 cm^{-1} (Tiwari et al. 2012; Gautam et al. 2016; Gautam et al. 2017).

FTIR spectra provide structural information e.g. functional groups, aggregation and alignment of chains and the level of doping. The spectra obtained have all the characteristics

peaks for PANI, as reported in the literature. Important stretching frequencies have been summarized and compared, given as (*c.f. Table D7*). IR spectrum of the PANI-HCl shows seven principal absorptions respective functional groups; $\sim 3500\text{ cm}^{-1}$, 1577 cm^{-1} , 1499 cm^{-1} , 1297 cm^{-1} , 1231 cm^{-1} , 1130 cm^{-1} , 806 cm^{-1} . Similar peaks were observed for other samples. They exhibited a slight shift in the peaks positions and intensity change, however. It can be attributed to effects of dopants and the structural modifications. In the spectra of PANI-HCl and PANI-Citric acid, the peak at 805 cm^{-1} is attributed to the out-of-plane bending of C-H and C-N ring stretching, whereas PANI-Lemon exhibited at 791 cm^{-1} . The peak shift toward lower energy indicates that lemon juice certainly affects the chain arrangements. The strong peak at 1130 cm^{-1} is attributed to N=Q=N structure for PANI-HCl and PANI-Citric acid, however this peak shifts to 1132 cm^{-1} for PANI-Lemon (fig. 8.3 A, C and E), attributed to feasible delocalization of pi electrons and good conductivity. Peak at 1231 cm^{-1} in PANI-HCl and PANI-Citric acid spectra is attributed to CCC ring in-plane deformation due to C-N stretching. This peak is shifted to higher energy 1238 cm^{-1} with higher intensity. Sharp and intense peak confirmed minimum distortion from its mean position. Benzenoid units of PANI chains bonded with each other through a network of weak hydrogen bonds. Such structure supported linear arrangement of PANI chains. PANI-Lemon shows a broad peak in the aromatic region due to dynamic proton exchange. Symmetrically arranged polyaniline chains exhibited minimum steric hindrance to the rapid proton exchange process. This result is also supported by NMR spectra (*c.f. D8*).

Stretching frequency 1297 cm^{-1} , attributed to C-N/ C=N, does not show any change in all the three samples. Relative higher peak intensities for N-quinoid than N-benzenoid rings (at 1568 cm^{-1} and at 1478 cm^{-1}) confirmed more quinoid units and suggested emeraldine

form of PANI. PANI-Lemon exhibited a sharp peak at $\sim 1650\text{ cm}^{-1}$ (CH ring in-plane bending), attributed to chains linearly arranged in a plane. No additional peaks or bands have appeared in the spectra of PANI-Lemon, which confirmed that most of the lemon juice contents could easily wash out from PANI matrix. The effects on the morphology persisted and the final material has no significant impurities, however. Comparative FTIR spectra for PANI samples, before and after catechol treatment, indicate the specific interactions with catechol (fig. 8.3 B, D, F). Significant peak shift is observed for aromatic units (1570 cm^{-1} to 1588 cm^{-1} , 1495 cm^{-1} to 1466 cm^{-1} , 1238 cm^{-1} to 1242 cm^{-1}). PANI-Lemon exhibited significant shift and decrease in intensity of peaks at frequencies 1588 cm^{-1} and 1141 cm^{-1} . It indicates that mainly quinoid rings participate in the interaction.

8.3.6 Electronic Spectra:

UV-Visible spectroscopy is an important technique to identify forms of PANI, variation in electronic structures, conformational changes and chain arrangement. The important electron absorption band are observed due to transition between HOMO to LUMO. $\sim 320\text{ nm}$ is attributed to $\pi\text{-}\pi^*$ transition in the benzenoid ring, $\sim 418\text{ nm}$ attributed to the polaron and bipolarons, $\sim 610\text{-}650$ - attributed to exciton formation and $\pi\text{-}\pi^*$ transition of quinoid rings and ~ 800 due to protonation of imine site. The dispersion of polaron bands between adjacent tetrameric units depends on the geometric arrangement of the polymer chains (Gautam et al. 2016; Gautam et al. 2017).

Electronic spectra reveal the structural changes and interaction of PANI with catechol, e.g. PANI-Lemon showed red-shift with higher intensity for the band at 353 nm (assigned to the $\pi\text{-}\pi^*$ transition) that indicates better charge delocalization and linear arrangements of

chains (*c.f.* D9). Linearly arranged PANI chains exhibit a better inter-chain charge transfer whereas twist defects of aromatic rings isolated the polarons of individual tetrameric units. PANI-Lemon exhibited changes in absorption band at 353 nm (assigned for pi-pi transition) which indicates that PANI-Lemon effectively interacts with catechol molecule (in accordance with FTIR analysis). Other than that, additional peaks appear at 277 nm and 271 nm, peak intensity decreased at 352 nm and 353 nm and higher absorption in the tail region (400 nm to 800 nm).

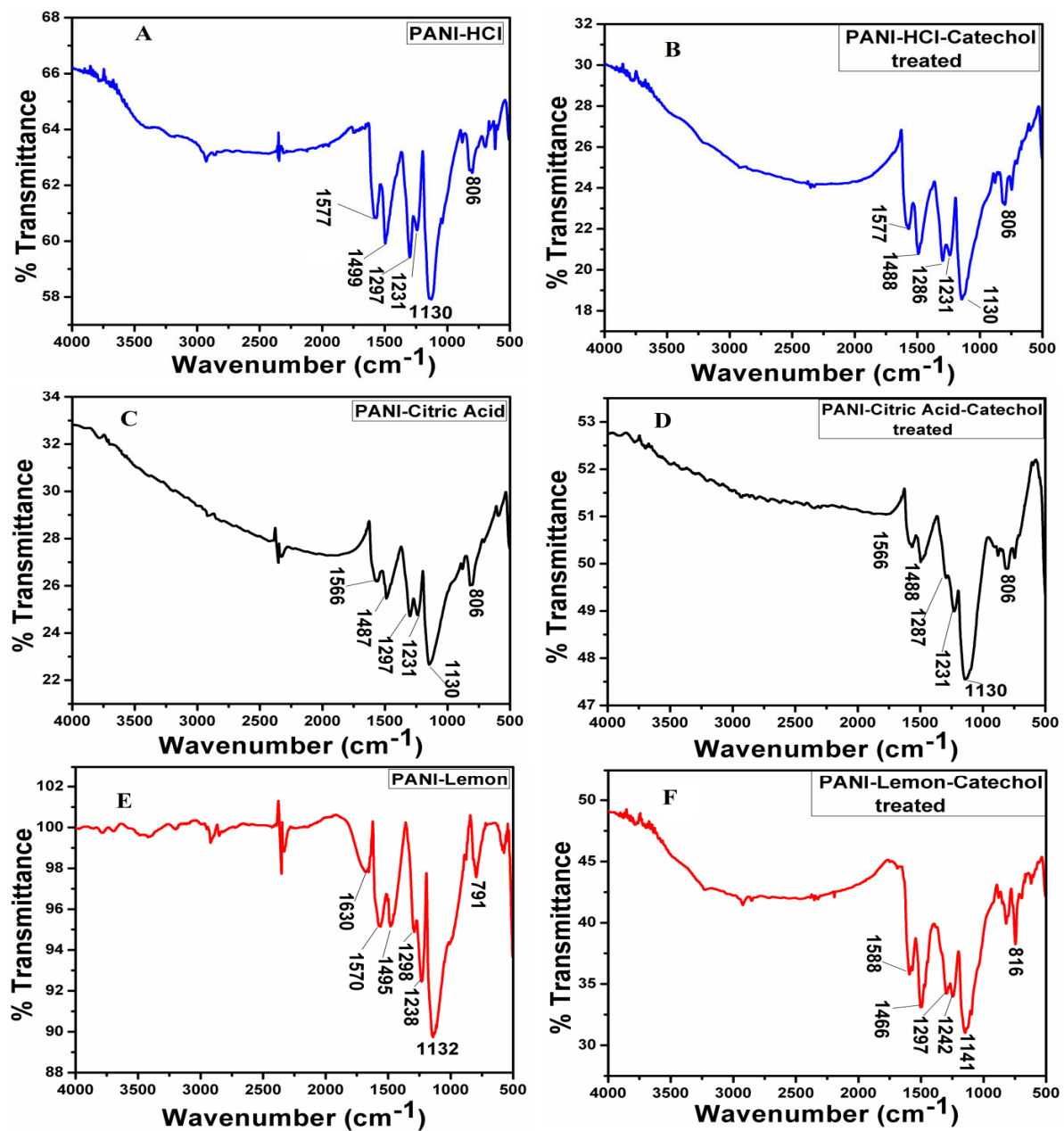


Fig. 8.3 FTIR spectra for (A) PANI-HCl, (C) PANI-Citric acid and (E) PANI-Lemon; After Catechol treatment (B) PANI-HCl, (D) PANI-Citric acid and (F) PANI-Lemon

8.3.7 Electrochemical Studies:

Electrochemical characterization of conducting polymers is of immense importance for applications such as batteries, corrosion protection, electrochemical sensors, electro-optic and electrochromic devices.

8.3.7.1 Cyclic Voltammetry:

CV analysis of PANI-HCl, PANI-Citric acid and PANI-Lemon was carried out at the rate 20 mV/s in the range (-400 mV to 800 mV) using three electrode system, Ag/AgCl as a reference electrode, PANI modified carbon paste as working and a platinum wire as counter electrode. CV of PANI and its composites depends on the nature of anionic dopant, the degree of protonation and oxidation state of polyaniline (Gautam et al. 2017; Gautam et al. 2016). In the acidic solution, cyclic voltammograms showed three important redox couples corresponding to following transitions: poly-leucoemeraldine/emeraldine salt, degradation products or over-oxidized products and poly-emeraldine salt/poly-pernigraniline. Anodic and cathodic scans are associated with doping/dedoping process of protons and anions respectively. Well shaped redox couples of PANI in 0.1 M HCl indicate its electroactivity and conductivity (fig. 8.5 A). PANI-Lemon showed higher peak currents than PANI-HCl and PANI-Citric acid that can be attributed to better charge transfer. In ordinary conditions, irregularly arranged PANI has some isolated redox sites, which do not participate in the charge-transfer process. The significant rise in peak current values justifies the impact of the lemon juice extract on the electrochemical properties of PANI.

Ionic bonds between NH^+ and anionic dopants stabilized the positive charge of PANI chains. The strength of these bonds is pH dependent and can easily break at higher and neutral pH. Small size dopant molecules/ions (such as chloride ion) could leach out from the

polymer matrix. To overcome this problem a variety of bulky anionic dopants have been used (Zhao et al. 2011; Maity et al. 2016; Kulkarni et al. 2004; Chowdhury et al. 2008). Figure 8.4 B shows the CV of the three PANI samples in phosphate buffer (pH 7.0), which indicate that PANI-Lemon is more electroactive than PANI-HCl and PANI-Citric acid. Symmetrically arranged PANI chains have suppressed deprotonation process, rapid proton exchange between primary and secondary amines and a network of hydrogen bonds (broad singlet for aromatic protons ~ 7 ppm in the NMR spectra of PANI-Lemon, confirms the symmetric arrangement of chain and rapid proton exchange reactions). For evaluation of proton doping/dedoping on the electrochemistry of the prepared materials, cyclic voltammograms were recorded in a series of working solutions, pH ranging from 1-7 (*c.f.* D10A, B and C). Anodic and cathodic peak currents decreased as the pH of the solution increased due to deprotonation.

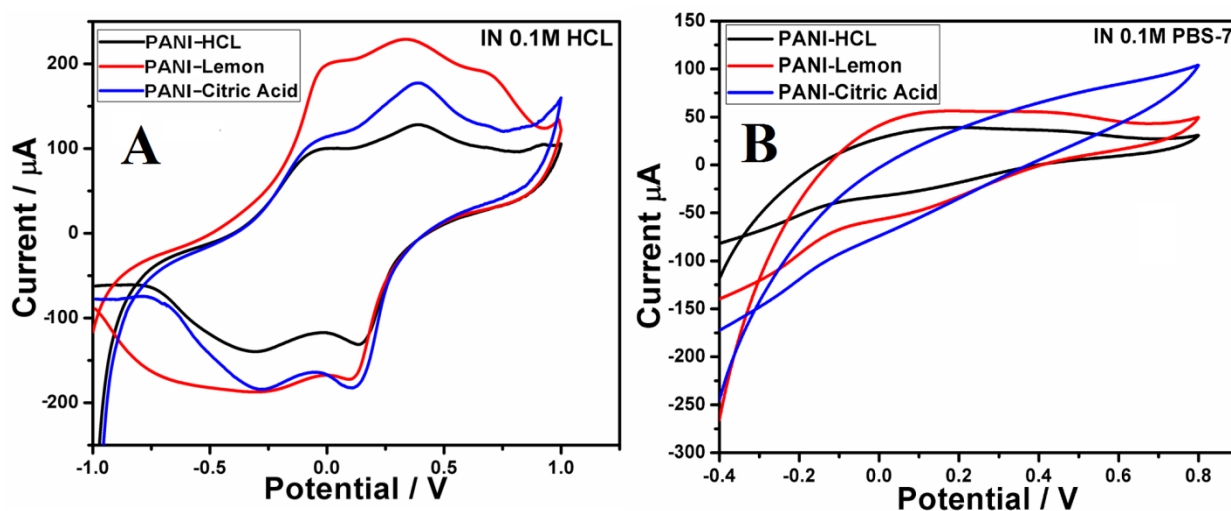


Fig. 8.4 Cyclic voltammogram of carbon paste electrode modified with PANI-HCl, PANI-Citric acid and PANI-Lemon, (A) in 0.1 M HCl (B) in PBS-7

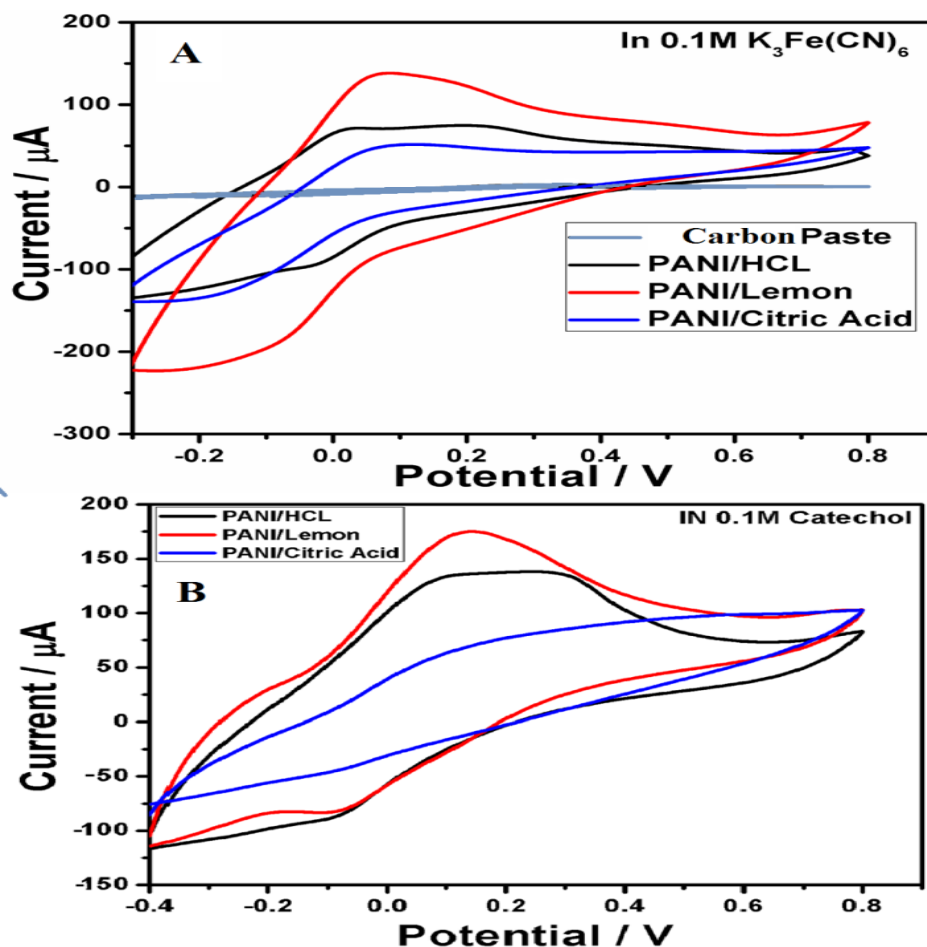


Fig. 8.5 Cyclic voltammogram of modified carbon paste electrode; blank, PANI-HCl and PANI-Lemon, PANI-Citric acid in PBS-7, (A) With 0.1 M potassium ferricyanide (B) With 0.1 M catechol

For comparing electroactivity, cyclic voltammograms were measured in the PBS solution (pH-7) at the scan rate of 20 mV/s, using Potassium ferricyanide as a redox marker (fig. 8.5A). No significant signal was observed at plane carbon paste electrode in the selected potential window. PANI-Lemon showed better redox behavior in terms of higher current and sharp peaks. So, we infer that modified electrodes are more sensitive to detect an electroactive species.

Similarly, the cyclic voltammetric response in the presence of catechol solution indicated that PANI-Lemon gives a better response for catechol than PANI-HCl and PANI-Citric acid (Fig. 8.5B). Although PANI-HCl has a larger surface area than PANI-Lemon, it exhibited lower current response. This interesting observation could be explained by considering the fact that the irregular arrangement of PANI chains has larger spatial charge impedance (leads to low conductivity). We herein propose that under similar protonation conditions, linear alignment of PANI chains is governing factor for higher peak current rather than surface area. This fact is also supported by cyclic voltammograms of PANI-Lemon(L) and PANI-HCL(H) in the absence/presence of catechol (*c.f.D11*). In spite of a significant difference in the surface area of two PANI samples, almost same cyclic voltammetric response was observed. The HR-SEM images have suggested that PANI-Lemon(L) has the longer nanorods than PANI-Lemon (H), but similar chain arrangement. We conclude that in the same protonation condition, the alignment of PANI chains is more significant than other structural parameters like size, shape and surface area. CV analysis suggests that PANI-Lemon is a better electrode material than PANI-HCl and PANI-Citric acid.

8.3.7.2 Alternative Current Electrochemical Impedance Spectroscopy (EIS):

EIS is an effective method to investigate the electronic features of surface-modified electrodes. The Nyquist plot was used to analyze the interfacial properties of PANI-Lemon, PANI-HCl and PANI-Citric acid in PBS solution at pH-1 (fig. 8.6A). The Nyquist diameter (real axis value at lower frequency intercept) reveals that PANI-Lemon modified electrode has lower charge transfer resistance (RCT) due to better electron-transfer, efficient anionic doping, porosity and linear alignment of chains. Alignment of chains and protonation are

major factors that decide the amount of charge transfer and conductivity of the system (Chowdhury et al. 2008). Although PANI-HCl has the smallest particle size and a larger surface area and greater protonation, it showed greater impedance due to a large number of inter-chain charge transfer. PANI-Citric acid has intermediate impedance due to more regular morphology (confirmed from HR-SEM images - some globular shape regular structure were observed). We inferred that PANI nano rods have guided spatial arrangement, extended charge delocalization, easy inter-chain charge transfer, minimum charge drainage and short diffusion path lengths. Primarily, conductivity depends upon the protonation level, but under similar protonation conditions, the spatial arrangement of chains could be a dominating factor.

Protonation is a very important factor that affects the bulk conductivity of PANI. So, we measured the impedance of PANI-Lemon in the solutions of different pH (fig. 8.6 B). Stable positive charge promotes the charge delocalization along the conjugated structures of polyaniline. Interface resistance was increased significantly in the solutions above pH-2, and sudden increment in resistance was observed at pH-6 due to deprotonation.

8.3.7.3 Detection of Catechol:

Polyaniline exists in three common oxidation states-leucoemeraldine base (fully reduced), emeraldine base (half-oxidized) and pernigraniline base (fully oxidized). Partially oxidized emeraldine salt behaves as a conductor, whereas fully reduced and oxidized forms act as an insulator (fig. 8.7C). Conducting form of PANI has alternate dynamic benzenoid-quinoid structures. The relative ratio of benzenoid and quinoid units is indicated from the corresponding intensity ratio in FTIR and NMR spectra.

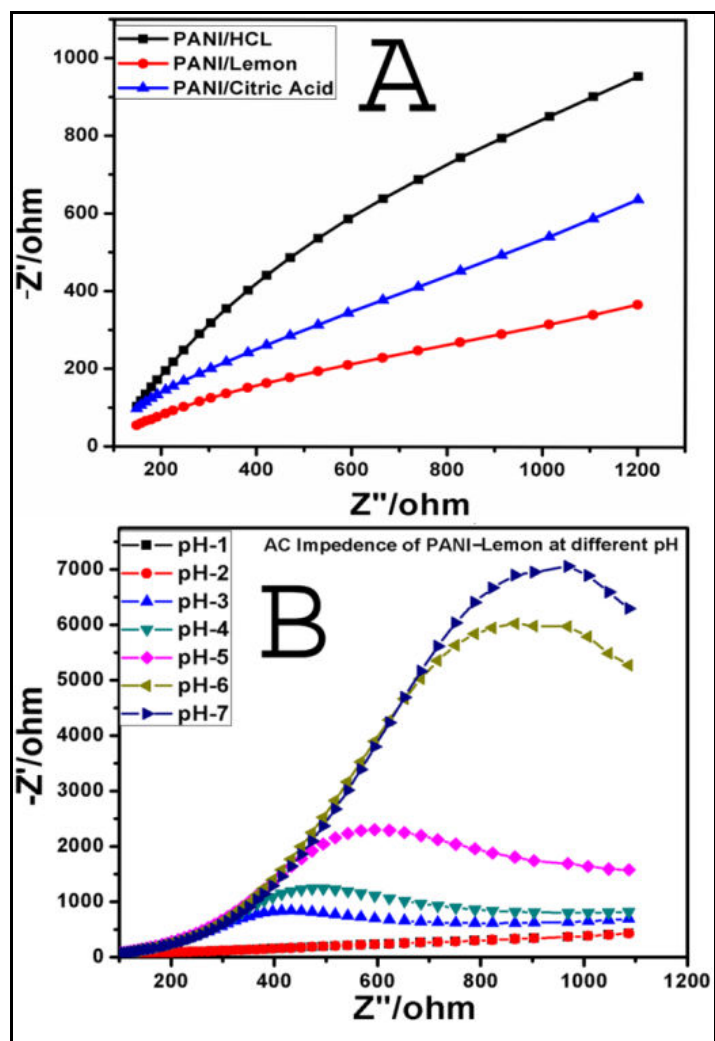


Fig. 8.6 Nyquist plots (A) PANI-HCl, PANI-Citric acid, PANI-Lemon modified carbon paste electrodes in dilute HCl (B) PANI-Lemon modified carbon paste electrodes in the PBS solution at different pH

Three important factors which control the conductivity of PANI are: (a) degree of protonation, (b) degree of oxidation and (c) spatial arrangement. Depending upon the degree of oxidation the electronic conductivity varies from insulating state to metallic. The stability of positive charge on the chain depends on the degree of protonation. In the neutral solution dedoping leads to the loss of conductivity and electroactivity. The delocalization of charge depends upon the length of the chain and proton exchange reactions. Conductivity and

structural changes associated with the proton exchange reactions have been examined by spectral analysis (Wang et al. 2010; Abdelkader et al. 2013). Catechol follows the reversible oxidation reaction involving two electrons and two protons exchanges. The protons released during oxidation process were accepted by the PANI, which led to an increase in conductivity and electroactivity. Linearly aligned polyaniline structure shows dominated proton exchange reaction and it could accept the protons released during catechol oxidation at the electrode surface. The three PANI samples PANI-HCl, PANI-Lemon and PANI-Citric acid were treated with 0.1 mM catechol solution and kept undisturbed for 6-8 hours and then separated out. UV-Visible spectra shows intense absorption peaks between 400-600 nm for PANI-Lemon, which indicates that PANI-Lemon could effectively interact with catechol and it catalyzes the formation of colored aromatic pigment “benzoquinone” (confirmed from red color for catechol solution obtained after treatment) (fig. 8.7 A, B).

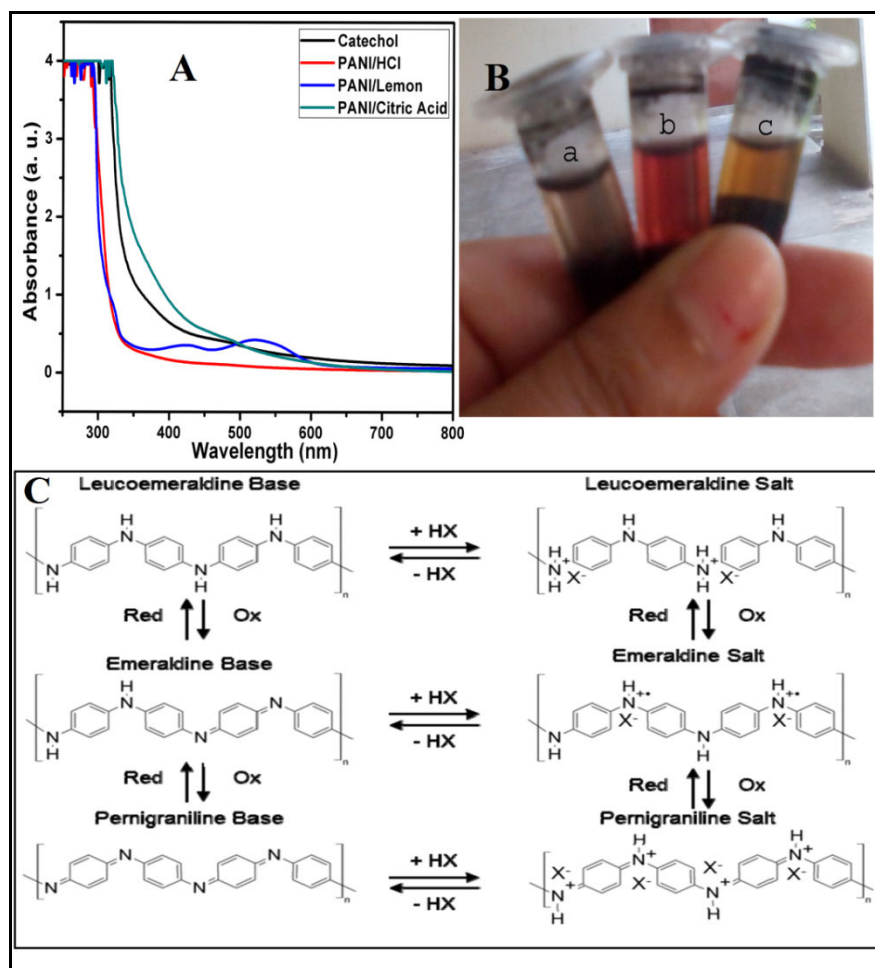
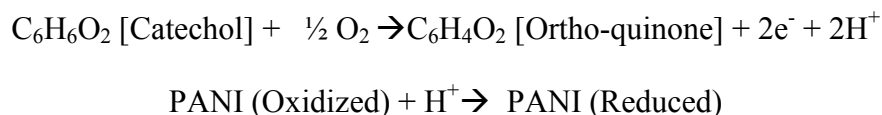
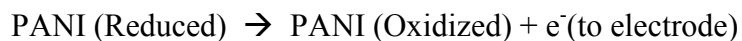


Fig. 8.7 (A) UV-Visible spectra of catechol (B) Photograph of catechol solution after treating with PANI (a) PANI-HCl (b) PANI-Lemon (c) PANI-Citric acid) (C) Different forms of polyaniline

The electrocatalytic activity of the PANI-Lemon modified electrode was investigated by cyclic voltammetry in the presence of different catechol solutions (5 μM -100 mM, PBS-7 as supporting electrolyte, scan rate 20 mV/s) (fig. 8.8A). Under mild conditions, catechol produce benzoquinone by quasi-reversible two-electron, two proton redox reaction. PANI-Lemon facilitates electrocatalytic oxidation of catechol at the electrode surface:





The anodic current increased continuously with every subsequent addition of catechol, attributed to catechol oxidation and higher protonation level of PANI (improved electroactivity and conductivity). The calibration plot (fig. 8.8B) indicates a linear range from 5 μM to 100 mM ($R^2 = 0.9773$), limit of detection 2.1 μM ($S/N=3$) and sensitivity of 49.68 $\mu\text{A mM}^{-1} \text{cm}^{-2}$. The limit of detection (LOD) was determined using the 3 SD/slope ratio, where SD is the standard deviation of the anodic current values of 10 responses in cyclic voltammograms of the blank. Thus, the present sensor has extended linear range, high sensitivity and low detection limit.

Catechol sensors have been fabricated by using many other materials such as, gold nano particle/cobalt hexacyanoferrate/SBA-15, poly(aniline-co-o-aminophenol), poly(N-vinyl pyrrolidone), PANI/polyacrylonitrile, silicon/tyrosinase, $\text{Fe}_3\text{O}_4/\text{PANI}/\text{chitosan}$, $\text{Fe}_3\text{O}_4\text{-SiO}_2$, MWCNTs/ MnO_2 , agarose-guar gum, graphene oxide/multi-walled carbon nanotubes/terthiophene, poly(malachite green)/MWCNTs, molecularly imprinted polymers, PANI/Ionic liquid, and DNA/graphene oxide (Alshahrani et al. 2014; Chandra et al. 2013; Chena et al. 2009; Lakshmi et al. 2009; Fu et al., 2014; Tang et al. 2008; Mu et al. 2006; Nazari et al. 2015; Sadeghi et al. 2015; Tembe et al. 2008; Sethuraman et al. 2013; Tan et al. 2010; Imato et al. 1993; Xue et al. 2002; Yan et al. 2015; Zhao et al. 2007). The performance of the proposed sensor was compared with some of the reported polyaniline based catechol sensors which has been summarized in Table-8.2.

Table 8.2 Comparison of performance of the proposed sensor with other polyaniline based catechol sensors

Electrode Material	Detection Limit and Sensitivity	Linear Range and Response Time	Reference
poly(aniline-co-p-aminophenol) -	0.8 μ M -	5 to 500 μ M -	Chena et. al. (28)
poly(aniline-co-o-aminophenol) -	- -	5-80 μ M & 10 Sec	Mu et. al. (32)
Polyaniline/Laccase	2.0 μ M	3.2 to 19.6 μ M -	Nazari et. al. (33)
Fe ₃ O ₄ / Polyaniline /Laccase/Chitosan Biocomposite	0.4 μ M & 126.76 μ AmM ⁻¹	0.5 to 80 μ M, & 8 Sec	Sadeghi et. al. (34)
Polyaniline/Polyphenol oxidase	- -	0.05 –165.5 μ M -	Sethuraman et.al. (36)
Polyaniline/Polyphenol oxidase	1.25–150 μ M -	0.3 to 51 μ M -	Tan et.al. (37)
Polyaniline/Polyacrylonitrile/ Polyphenol oxidase	- 2.03 AM ⁻¹ cm ⁻²	0.05 –7.5 μ M -	Xue et. al. (39)
Polyaniline nano rods	2.1 μ M & 49.68 μ A μ M ⁻¹ cm ⁻²	5 μ M to 100 mM 2 Sec	(Current work)

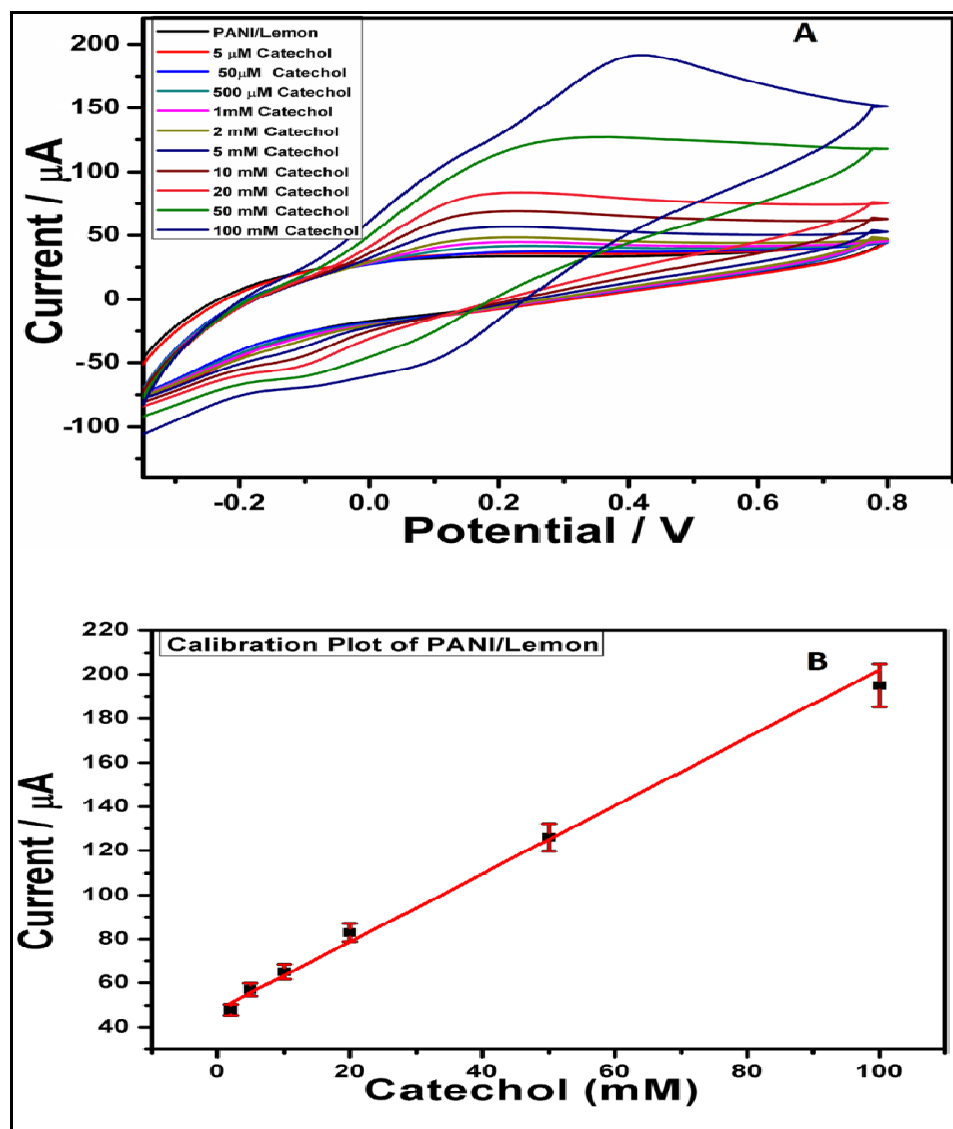


Fig. 8.8 (A) Cyclic Voltammograms of PANI-Lemon modified carbon paste electrode in the presence of different concentration of catechol in PBS-7, (B) Calibration plot.

8.3.7.4 Differential Pulse Voltammetry And Chronoamperometry:

DPV and chronoamperometry of PANI-Lemon were carried out in PBS-7.0 using different concentrations of catechol (*c.f. DI2*). It is interesting to note that the blank experiment with PANI-Lemon showed two peaks at potential ~ 30 mV and ~ 320 mV, but after the addition of catechol, a third peak was observed at ~ 600 mV. With further addition of catechol, there was

an increment of current at all three peak potential, however, the third peak shows the relatively higher current response. It is inferred that the newly generated redox center on PANI-Lemon is more sensitive for catechol detection.

Chronoamperometric experiments were performed at single potential step, + 0.5 V vs. Ag/AgCl and the resultant current was measured with respect to time. PANI-Lemon exhibited catalytic oxidation of catechol and anodic current increased with subsequent addition. The faradaic chronoamperometric responses were in good agreement with the CV measurements.

8.3.7.5 Response of Other Analytes:

The cyclic voltammetric responses of different analyte using PANI-Lemon modified electrode in PBS-7 were also observed (*c.f.* D13). The response for other interfering substances was quantitatively plotted as the percentage increase in the anodic current with respect to blank peak current (fig. 8.9). It was found that catechol exhibited higher anodic peak current response. The material showed good response for ascorbic acid and phenol too.

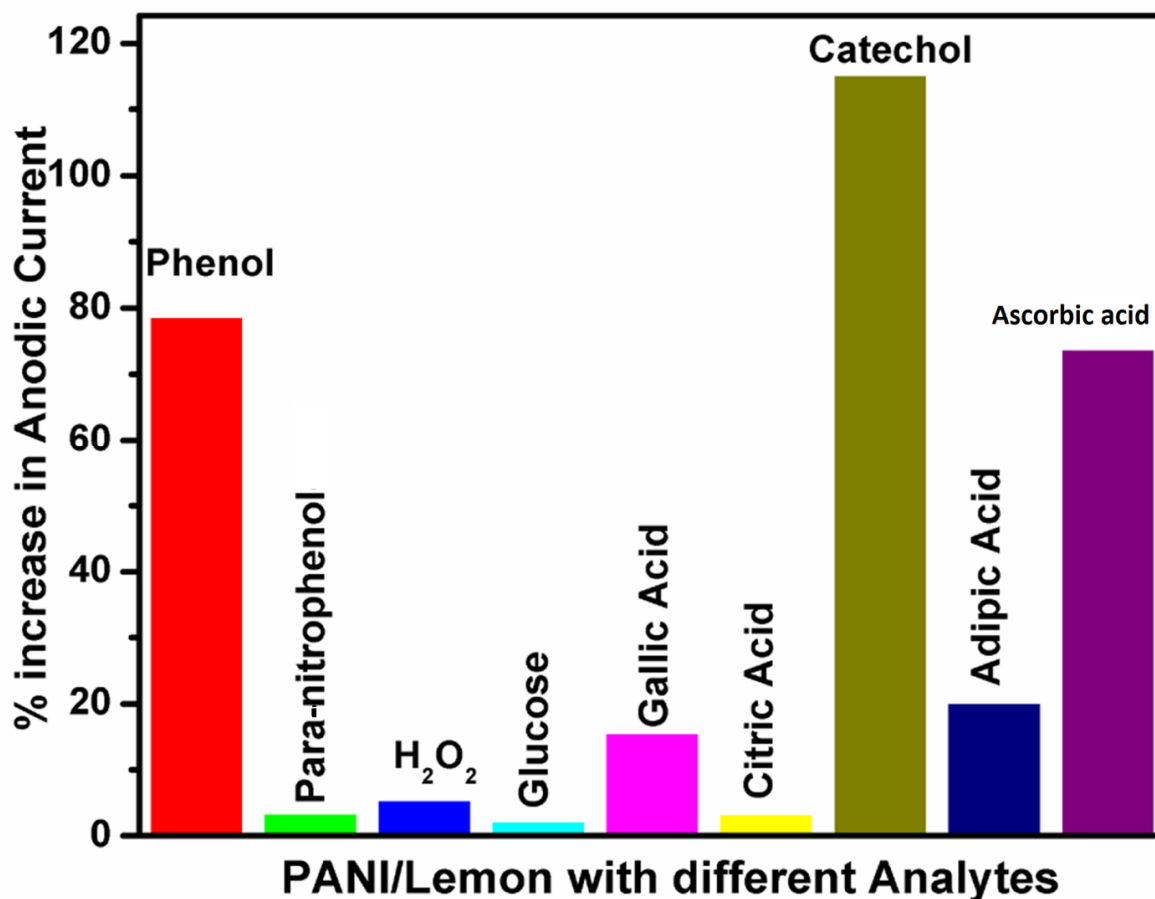


Fig. 8.9 Increment of anodic peak current in the CV response of different analytes on PANI-Lemon modified carbon paste electrode

8.4 Conclusions:

On the basis of the above results and discussion, we have drawn following important conclusions:

1. Natural extract assisted synthesis could manipulate the nanostructures having novel properties.
2. The important aspects and presumptions of “Multi-component Template Effects” have been discussed. This concept can be potentially implemented to synthesize other polymers and nanoparticles. It is possible that this template like effect may be produced

due to the combined impact of several molecules. The synergistic effect of different molecules is a matter of further research.

3. Lemon juice assisted polymerization is a cost-effective and environment-friendly method for the synthesis of PANI. Molecules of lemon juice produce template like effects on the morphology of PANI. The polymerization reaction in lemon juice followed sluggish kinetics and resulted in longer induction period due to lower pKa value of lemon juice. This condition provides good opportunity for self-assembling of PANI chains.

4. SEM, HR-SEM, TEM and AFM images confirm the formation of rod shape nanostructures (dimension: diameter \sim 100 nm, length \sim 300 - 600 nm). FTIR and UV-Visible spectra provided valuable structural information. The distinct molecular structure of PANI-Lemon is confirmed from the intensity ratio of peaks for benzenoids and quinoids units and blue shift for N=Q=N stretching vibrations. PANI-Lemon is found to be superior to PANI-HCl and PANI-Citric acid, in terms of more quinoid units, linear alignment of the chains, extended dispersion of polaron bands, higher conductivity and better electroactivity. XRD and electron diffraction patterns of PANI-Lemon support polycrystalline structure, this confirms that there is a regular arrangement of chains in the rod-shaped nanostructures.

We have proposed that in the similar protonation conditions, (i) spatial arrangement of chains is the dominating factor which decides conductivity and electroactivity of PANI (due to better inter-chain charge transfer) and (ii) the alignment of chains is more significant structural parameter than size and surface area.

5. PANI-Lemon modified carbon paste capillary electrode was successfully used for catechol sensing. On interacting with catechol, it generates new redox-active sites that are more sensitive to catechol. The developed catechol sensor exhibited high sensitivity ($49.68 \mu\text{A}\mu\text{M}^{-1}$)

Chapter 8

$^1\text{cm}^{-2}$), wide linear concentration range (5 μM -100 mM), low detection limit (2.1 μM) and lower response time (2s). Thus, PANI-Lemon is a better electrode material than PANI-HCl and PANI-Citric acid due to large surface area, porous architecture, low interfacial resistance, and good electro-catalytic property.